*Journal of Statistical Physics, Vol. 59, Nos. 5/6, 1990*

# The Mechanism of the Increase of the Generalized Dimension of a Filtered Chaotic Time Series

**A. Chennaoui,[1] J. Liebler,[1] and H. G. Schuster[2]**

*Received September 14, 1989*

The determination of the attractor dimension from an experimental time series may be affected by the influence of filters which are incorporated into many measuring processes. While this is expected from the Kaplan–Yorke conjecture, we show that for one-dimensional maps a weak filter can induce a self-similarity which is responsible for the increase of the Hausdorff dimension. We are able to calculate the increase of the generalized dimension $D_q$ for the filtered time series of the logistic map $x_{t+1} = rx_t(1-x_t)$ at $r=4$ analytically.

**KEY WORDS:** Frobenius–Perron integral equation; filtered time series of one-dimensional maps; Liapunov exponent; Hausdorff dimension; generalized dimension $D_q$.

## 1. INTRODUCTION

Chaotic signals are frequently characterized by evaluating the fractal dimension of the underlying strange attractor, which is reconstructed in a suitable embedding space.[1] A variety of factors affect the determination of its dimension. One of these is the bandwidth of a filter which could be incorporated inevitably into the measuring instrument. Badii and Politi[2,3] showed by means of the Kaplan–Yorke conjecture and numerically that the dimension of a low-dimensional chaotic time series can be raised if it is filtered by a low pass filter of first order.

We investigate the filtered time series of the logistic map and show analytically how its dimension increases. The two-dimensional invariant density of the coupled system consisting of the logistic map and the filter

[1] Institut für Theoretische Physik, Universität Frankfurt, D-6000 Frankfurt-Main, Federal Republic of Germany.

[2] Institut für Theoretische Physik und Sternwarte, Universität Kiel, D-2300 Kiel 1, Federal Republic of Germany.



0022-4715/90/0600-1311$06.00/0 

is calculated in a perturbation-theoretic way in the limit of a weak filter. The resulting density is in excellent agreement with numerical results obtained with a statistical method in which the two-dimensional phase space is divided into squares and the number of intersections of the trajectory with each square is counted. The analytic form of the density allows us also to calculate the generalized dimension[1] $D_q$ analytically. We show that for arbitrary one-dimensional maps a weak filter always induces self-similarity due to which the Hausdorff dimension increases.

## 2. CALCULATION OF THE INVARIANT DENSITY $\rho(x, z)$

The influence of a low-pass filter of first order on a signal $x_i$ which appears at discrete times $i$ can be modeled via

$$z_{i+1} = \varepsilon z_i + (1-\varepsilon) x_{i+1} \tag{2.1}$$

Here we assumed that $x_i$ is confined to the interval $[0, 1]$ and we scaled $z_i$ to the same interval by introducing a factor $(1-\varepsilon)$. The $z_i$ is the filtered signal and $\varepsilon = e^{-\eta}$, where $\eta$ is the bandwidth of the filter.[2,3] For the logistic map at $r = 4$

$$x_{i+1} = f(x_i) = 4x_i(1-x_i) \tag{2.2}$$

the invariant density is given by[1]

$$\bar{\rho}(x) = \frac{1}{\pi[x(1-x)]^{1/2}} \tag{2.3}$$

The two-dimensional density $\rho(x, z)$ obeys the Frobenius–Perron equation

$$\rho(x, z) = \int_0^1 dz' \int_0^1 dx'\, \delta(x - 4x'(1-x'))\, \delta(z - \varepsilon z' - (1-\varepsilon)x)\, \rho(x', z')$$

$$= \frac{1}{4\varepsilon(1-x)^{1/2}} \sum_{j=1,2} \rho\left(g_j(x), \frac{z-(1-\varepsilon)x}{\varepsilon}\right) \equiv F[\rho]_{(x,z)} \tag{2.4}$$

where

$$g_j(x) = \frac{1-(-1)^j (1-x)^{1/2}}{2}, \qquad j = 1, 2 \tag{2.5}$$

and $(1-\varepsilon)x \leqslant z \leqslant \varepsilon + (1-\varepsilon)x$. For $\varepsilon = 0$ the two-dimensional invariant density is given by

$$\rho^{(0)}(x, z) = \bar{\rho}(x)\, \delta(z - x) \tag{2.6}$$

Equation (2.4) can be solved iteratively via

$$\rho^{(n)}(x, z) = F[\rho^{(n-1)}]_{(x,z)} \tag{2.7}$$

For arbitrary $n \geqslant 1$ the invariant density $\rho^{(n)}$ is given by

$$\rho^{(n)}(x, z)$$

$$= 2^{-n} \bar{\rho}(x) \sum_{j_1, j_2, \ldots, j_n = 1, 2} \delta\left( z - (1-\varepsilon)x - \sum_{i=1}^{n} \varepsilon^i (1-\varepsilon)^{1-\delta_{i,n}} g_{j_i}(g_{j_{i-1}}(\ldots(g_{j_1}(x))\ldots)) \right)$$

$$\equiv 2^{-n} \bar{\rho}(x) \sum_{m=1}^{2^n} \delta(z - v_m^{(n)}(x)) \tag{2.8}$$

The intricate functions in the argument of the $2^n$ $\delta$-functions in $\rho^{(n)}$ are denoted by $v_m^{(n)}(x)$ $(m = 1, 2, \ldots, 2^n)$. If all powers $\varepsilon^n$ which appear in $\rho^{(n)}$ are replaced by zero, it reduces to $\rho^{(n-1)}$. Therefore the iteration of $n$th order will give a solution which is correct up to the $n$th power of $\varepsilon$.

We find explicitly

$$\rho^{(0)}(x, z) = \frac{1}{\pi[x(1-x)]^{1/2}} \delta(z - x) \tag{2.9a}$$

the first iteration yields

$$\rho^{(1)}(x, z) = \frac{1}{2\pi[x(1-x)]^{1/2}} \left\{ \delta\left( z - (1-\varepsilon)x - \varepsilon\left( \frac{1}{2} + \frac{1}{2}(1-x)^{1/2} \right) \right) + \delta\left( z - (1-\varepsilon)x - \varepsilon\left( \frac{1}{2} - \frac{1}{2}(1-x)^{1/2} \right) \right) \right\} \tag{2.9b}$$

and the second iteration yields

$$\begin{aligned} \rho^{(2)}(x, z) = \frac{1}{4\pi[x(1-x)]^{1/2}} \Bigg\{ & \delta\left( z - (1-\varepsilon)x - \varepsilon(1-\varepsilon)\left( \frac{1}{2} + \frac{1}{2}(1-x)^{1/2} \right) - \varepsilon^2\left( \frac{1}{2} + \frac{1}{2}\left[ \frac{1}{2} - \frac{1}{2}(1-x)^{1/2} \right]^{1/2} \right) \right) \\ & + \delta\left( z - (1-\varepsilon)x - \varepsilon(1-\varepsilon)\left( \frac{1}{2} + \frac{1}{2}(1-x)^{1/2} \right) - \varepsilon^2\left( \frac{1}{2} - \frac{1}{2}\left[ \frac{1}{2} - \frac{1}{2}(1-x)^{1/2} \right]^{1/2} \right) \right) \\ & + \delta\left( z - (1-\varepsilon)x - \varepsilon(1-\varepsilon)\left( \frac{1}{2} - \frac{1}{2}(1-x)^{1/2} \right) - \varepsilon^2\left( \frac{1}{2} + \frac{1}{2}\left[ \frac{1}{2} + \frac{1}{2}(1-x)^{1/2} \right]^{1/2} \right) \right) \\ & + \delta\left( z - (1-\varepsilon)x - \varepsilon(1-\varepsilon)\left( \frac{1}{2} - \frac{1}{2}(1-x)^{1/2} \right) - \varepsilon^2\left( \frac{1}{2} - \frac{1}{2}\left[ \frac{1}{2} + \frac{1}{2}(1-x)^{1/2} \right]^{1/2} \right) \right) \Bigg\} \end{aligned} \tag{2.9c}$$

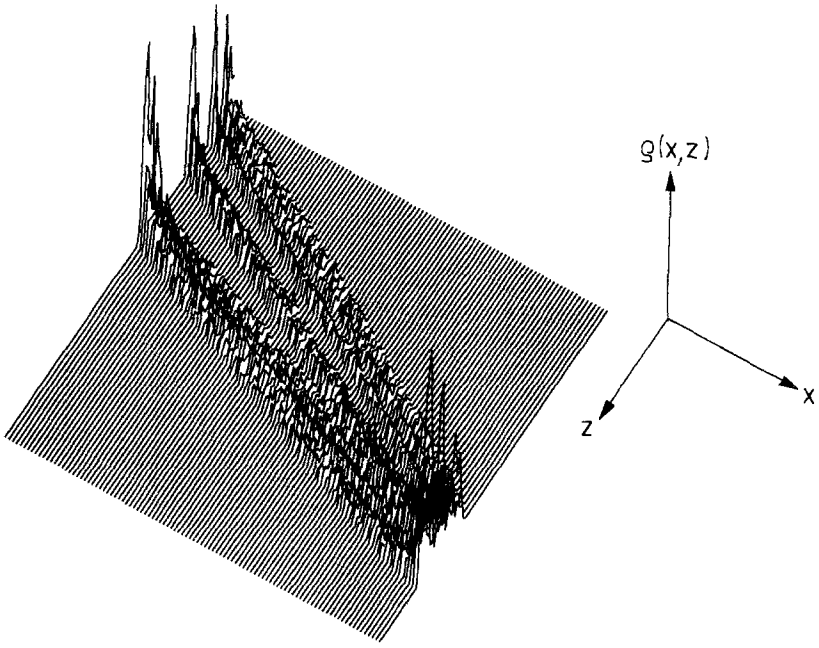


Fig. 1. The invariant density $\rho(x, z)$ computed with the statistical method for $\eta = 0.7$.

The results of the statistical method explained in the introduction (Fig. 1) and the perturbational method (Fig. 2) are compared for $\eta = 0.7$. For the perturbational method $\rho^{(10)}$ has been used. The $\delta$-functions appearing there have been approximated by Gaussians.

## 3. THE STRUCTURE OF THE ATTRACTOR

The image of the attractor in the $x$–$z$ plane is generated by the zeros of the arguments of the $\delta$-functions of the specific approximations. In Fig. 3 the attractor generated by $\rho^{(1)}$ (Fig. 3a) and $\rho^{(2)}$ (Fig. 3b) are depicted; they are called first- and second-order attractors for brevity. We chose $\eta = 2$ for these plots, i.e., $\varepsilon \simeq 0.14$ and $\varepsilon^2 \simeq 0.02$. The first-order attractor consists of two lines in the plane the distance of which is of order $\varepsilon$. They have been created from the solitary line of the zeroth-order attractor by the iteration $\rho^{(1)} = F[\rho^{(0)}]$. Calculating the second-order attractor, each line of the first-order attractor is split into two lines separated by a distance of order $\varepsilon^2$. Provided $\varepsilon$ is small enough, the second-order attractor consists of two pairs of lines the mean distance of which is of order $\varepsilon$. This process can be continued by iteration such that the $n$th-order attractor consists of $2^n$ lines, which are arranged in a self-similar pattern. This self-similarity is

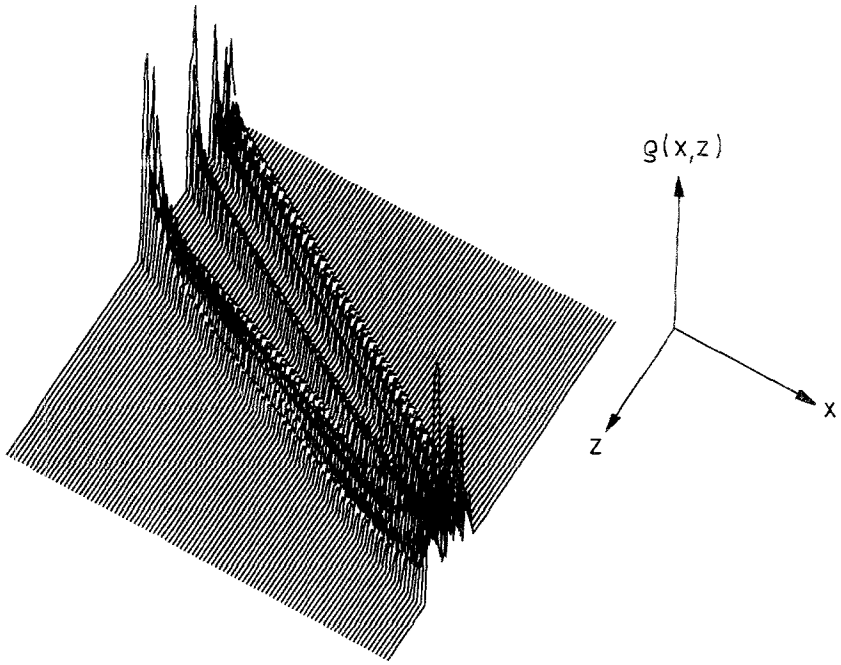


Fig. 2. The invariant density $\rho(x, z)$ computed with the perturbational method for $\eta = 0.7$.

characterized by the fact that each line of the attractor which can be resolved at a given scale will split into two lines if the scale is magnified by $1/\varepsilon$. This line doubling is a consequence of the properties of the logistic map [Eq. (2.2)], i.e., the inverse map consists of two branches.

If $\varepsilon$ exceeds a critical value $\varepsilon_c$, the self-similarity of the attractor vanishes and it becomes quasi-two-dimensional. This can be understood from a simple consideration, which is illustrated by the schematic diagram in Fig. 4. The straight lines are two adjacent lines of the $n$th-order attractor. The dashed lines are the corresponding four lines of the $(n+1)$th-order attractor; each pair is positioned symmetrically around the correspondent line of the $n$th-order attractor. If the distance between line $C$ and line $D$, which is denoted by $\overline{CD}$, becomes lower than the sum $\overline{BC} + \overline{DE}$, the self-similar pattern must vanish. Together with

$$\overline{BC} = \overline{DE} = \tfrac{1}{2}\varepsilon^{n+1} \qquad \text{and} \qquad \overline{CD} = \varepsilon^n - \varepsilon^{n+1} \tag{3.1}$$

this gives for $\varepsilon_c$ the condition

$$\overline{BC} + \overline{DE} = \overline{CD} \to \varepsilon_c = 0.5 \tag{3.2}$$

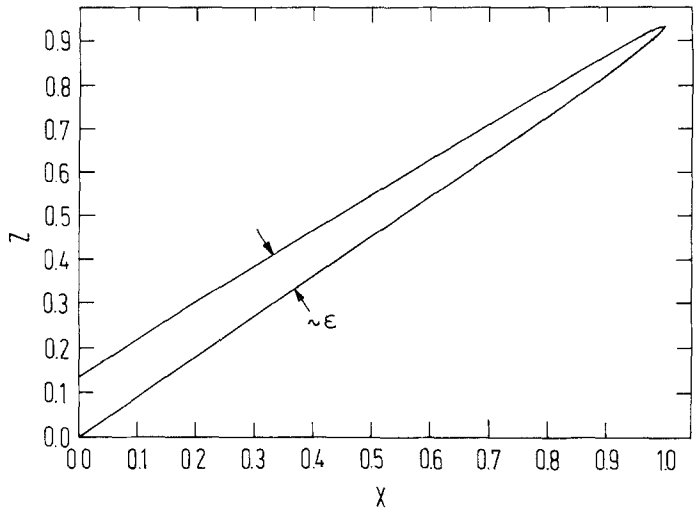


(a)

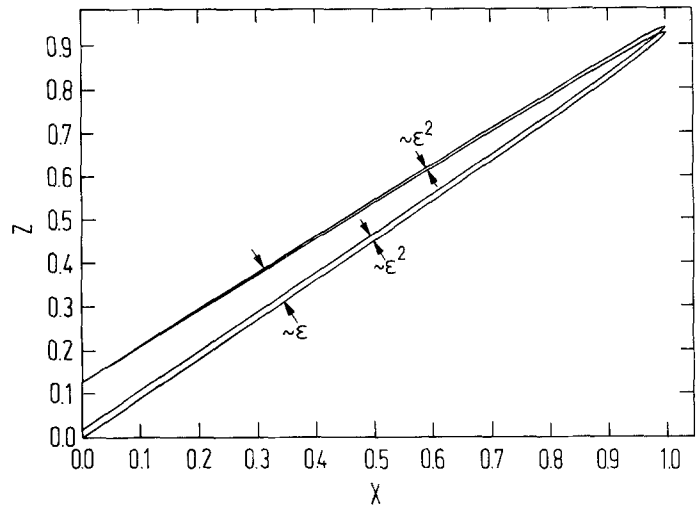


(b)

Fig. 3. (a) The first-order attractor and (b) the second-order attractor for $\eta = 2$.

There is an equivalent possibility to generate the $n$th-order attractor. Equations (2.1) and (2.2) can be written in vectorial notation

$$\begin{pmatrix} x_{i+1} \\ z_{i+1} \end{pmatrix} = \mathbf{G}((x_i, z_i)) \tag{3.3}$$

The $n$th iterate of the two-dimensional map $\mathbf{G}$ is denoted by $\mathbf{G}^n$, i.e.,

$$\mathbf{G}^n((x, z)) = \mathbf{G}(\mathbf{G}(\ldots(\mathbf{G}((x, z)))\ldots)) \quad n\text{-times} \tag{3.4}$$

The zeroth-order attractor is the line $\gamma^{(0)} = \{(x, z) \mid z = x,\ x \in [0, 1]\}$. The $n$th-order attractor is the image of $\gamma^{(0)}$ under the map $\mathbf{G}^n$, which can be seen as follows. The point $(a, a)$ belongs to $\gamma^{(0)}$ for $0 < a < 1$. The value $\mathbf{G}^n((a, a))$ is given by

$$\mathbf{G}^n((a, a)) = \begin{pmatrix} f^n(a) \\ (1-\varepsilon) f^n(a) + (1-\varepsilon)\,\varepsilon f^{n-1}(a) + \cdots + (1-\varepsilon)\,\varepsilon^{n-1} f(a) + \varepsilon^n a \end{pmatrix} \tag{3.5}$$

where $f^n$ is the $n$th iterate of the map $f$ [Eq. (2.1)]. The inversion of the equation $b = f^n(a)$ gives $a$ as a function of $b$. This inversion is not unique, because there are $2^n$ different branches. If one of the possible solutions is inserted into the vector on the right-hand side of Eq. (3.5), the zero of the argument of one of the $\delta$-functions of Eq. (2.8) is recovered. This proves the assertion. From this representation one recognizes that the $n$th-order attractor consists of the single curve $\gamma^{(n)} = \{\mathbf{G}^n((x, z)) \mid z = x,\ x \in [0, 1]\}$, which can have intersections with itself.

Figure 5 shows the attractor in the phase space corresponding to the

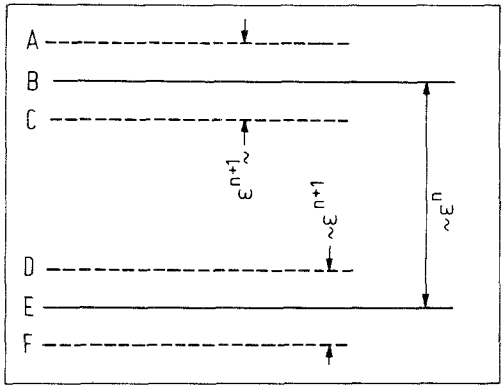


Fig. 4. Schematic diagram demonstrating the topological properties of the attractor.

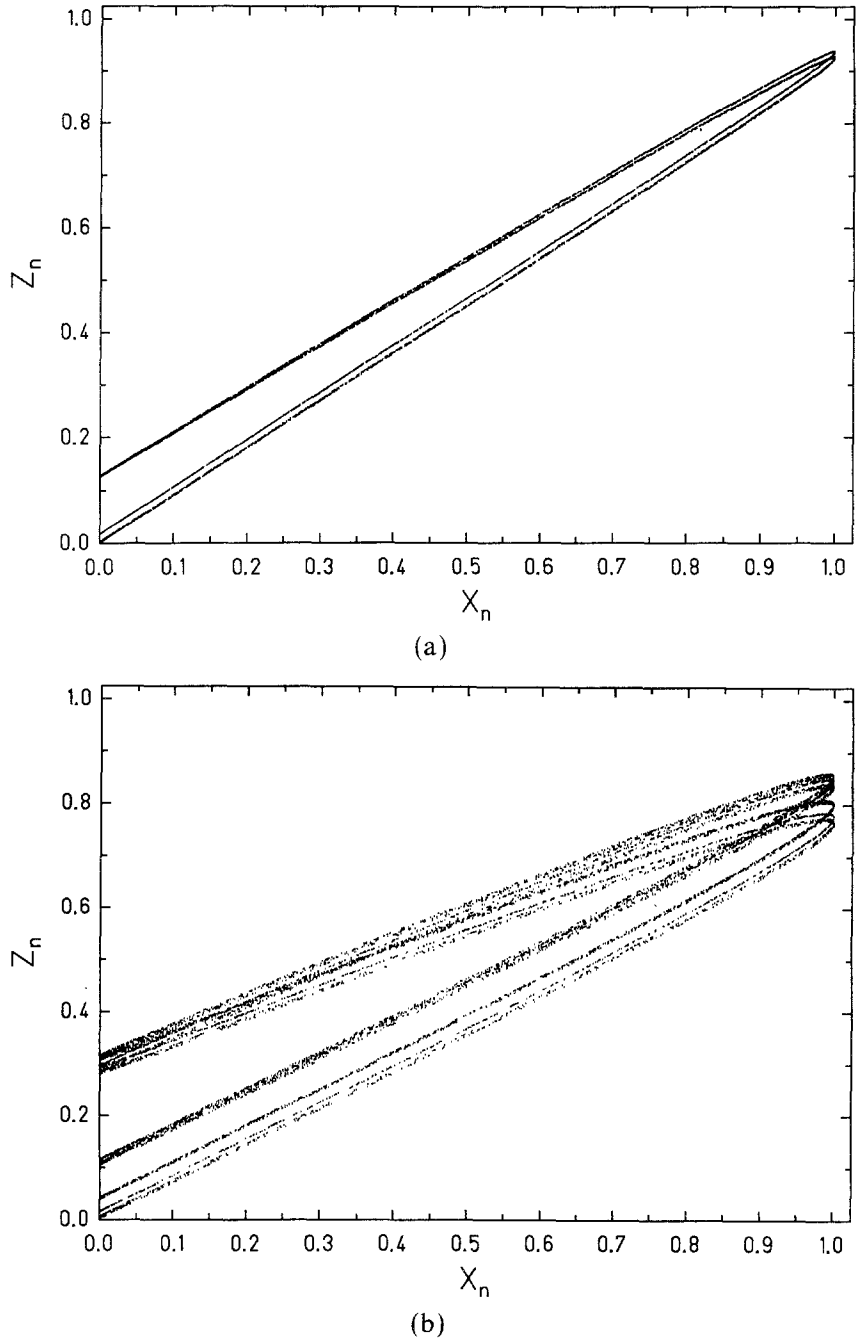


Fig. 5. The attractor ($z_n$ versus $x_n$) for the values (a) $\eta = 2$, (b) 1, and (c) 0.1.

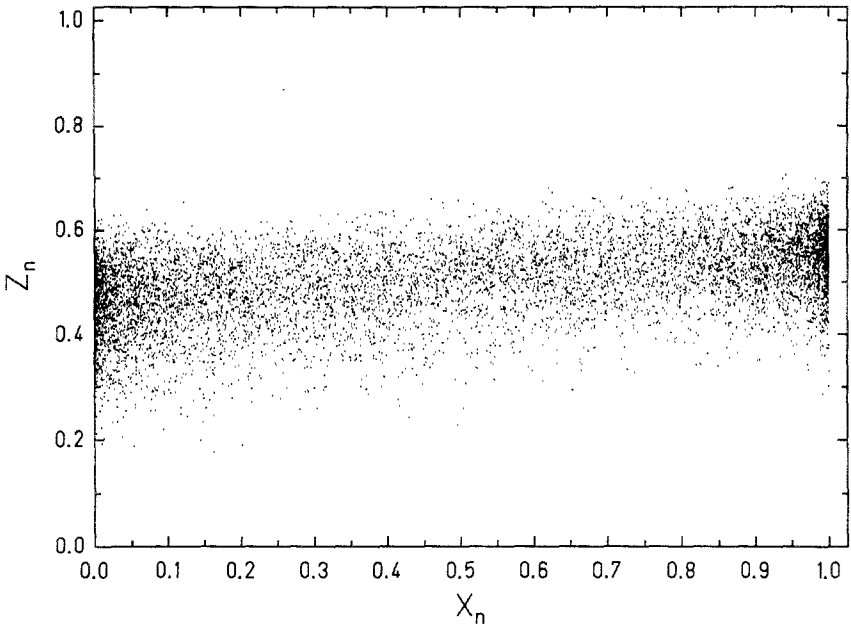


(c)

Fig. 5. (*Continued*)

values $\eta = 2$ (Fig. 5a), $\eta = 1$ (Fig. 5b), and $\eta = 0.1$ (Fig. 5c). These pictures are obtained by iterating Eqs. (2.1) and (2.2) and plotting $z_{i+1}$ versus $x_{i+1}$. The shrinkage of the attractor in the $z$ direction for decreasing $\eta$ is due to the normalization $(1-\varepsilon)$ in Eq. (2.1). For $\eta = 0.1$ the dimension of the attractor is visibly two.

## 4. CALCULATION OF THE HAUSDORFF DIMENSION $D_0$

The Hausdorff dimension $D_0$ is calculated from

$$D_0 = \lim_{l \to 0} -\frac{\ln N(l)}{\ln l} \tag{4.1}$$

$N(l)$ is the minimum number of squares of side length $l$ needed to cover the attractor. If $\varepsilon$ is smaller than $\varepsilon_c$, the attractor is self-similar and the Hausdorff dimension can be calculated in the following way. Only those lines divided from each other by a mean distance greater than $l$ can be

resolved. The smallest distance between two adjacent lines of the $n$th-order attractor is $\varepsilon^n$. If $n$ is chosen such that

$$\varepsilon^{n(l)} \sim l \tag{4.2}$$

holds, then the distribution of squares which cover the $n(l)$th-order attractor cover the whole attractor of the system (3.2), too. The $n(l)$th-order attractor consists of $2^{n(l)}$ lines. The smallness of $\varepsilon$ ensures that most squares hit only one line of the $n(l)$th-order attractor; therefore an upper bound $N^>$ for the number of squares which cover the attractor is

$$N^>(l) \sim \frac{2^{n(l)}}{l} \tag{4.3}$$

The number $lN^>(l)$ is proportional to the length of the curve $\gamma^{(n)}$. Taking into account that $\varepsilon = \exp(-\eta)$,

$$D_0 \leqslant \lim_{l \to 0} -\frac{\ln(2^{-\ln(l)/\eta}/l)}{\ln l} = 1 + \frac{\ln 2}{\eta} \tag{4.4}$$

follows. In Eq. (4.3) we have counted too many squares. In order to have a lower bound for $N(l)$, we substract the number of intersections of two lines (see, for example, Fig. 5b) for all possible pairings. A pair of lines will intersect once at most; therefore, the maximum number of intersections is given by $2^{n-1}2^n - 1 \simeq 2^{2n-1}$. For a lower bound of the Hausdorff dimension this yields

$$\begin{aligned} D_0 &\geqslant \lim_{l \to 0} -\frac{\ln(2^{-\ln(l)/\eta}/l - 2^{-1-2\ln(l)/\eta})}{\ln l} \\ &= 1 + \frac{\ln 2}{\eta} - \lim_{l \to 0} \frac{\ln(1 - l^{1-\ln(2)/\eta}/2)}{\ln l} \end{aligned} \tag{4.5}$$

If $\eta$ is greater than ln 2 (i.e., $\varepsilon < \varepsilon_c$), the lower bound of $D_0$ equals the upper bound of $D_0$.

The lower bound for $\eta$ for the applicability of Eq. (4.4) can be derived alternatively with the following approach: The number $N(l)$ cannot grow faster than $1/l^2$, this yields the inequality

$$\frac{2^{-\ln(l)/\eta}}{l} < \frac{1}{l^2} \tag{4.6}$$

which gives in the limit $l \to 0$ the condition

$$\eta > \ln 2 \tag{4.7}$$

which is consistent with the condition from Eqs. (4.5) and (3.2). If $\eta$ is smaller than the number ln 2, the dimension of the attractor is two. The complete formula for the Hausdorff dimension therefore becomes

$$D_0 = 1 + \frac{\ln 2}{\max(\eta, \ln 2)} \tag{4.8}$$

Considering that ln 2 is the positive Liapunov exponent for the logistic map (2.2), formula (4.8) proves the Kaplan–Yorke conjecture[5,6] in this specific case.

In Fig. 6 the Hausdorff dimension of the attractor is plotted versus the filter parameter $\eta$. The straight line is calculated from Eq. (4.8). The filled circles are obtained by evaluating the correlation function $C_q^m(l)$ for $q=0$ numerically. See ref. 4 for the explicit form of the function $C_q^m(l)$.

The graph $C_0^m(l)$ plotted versus $\ln l$ sometimes exhibits oscillations (Fig. 7), which are due to the self-similarity of the attractor. In our specific example the period of the oscillations is $\eta$. This can be understood from the following consideration. We discuss the formula

$$D_0(l) = \frac{\ln N(l)}{\ln(1/l)} \tag{4.9}$$

which can be interpreted as the dimension of the attractor, measured with squares of side length $l$. From (4.2) one obtains the equation

$$n(l) = \frac{\ln(1/l)}{\eta} \tag{4.10}$$

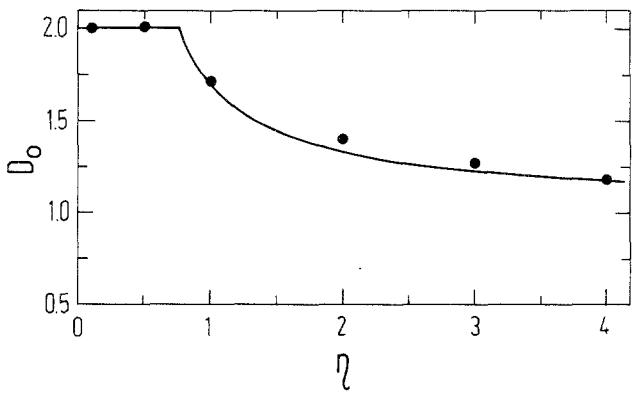


Fig. 6. Plot of $D_0$ versus $\eta$. The straight line is the theory and the points are calculated by the correlation method for $q=0$.[4]

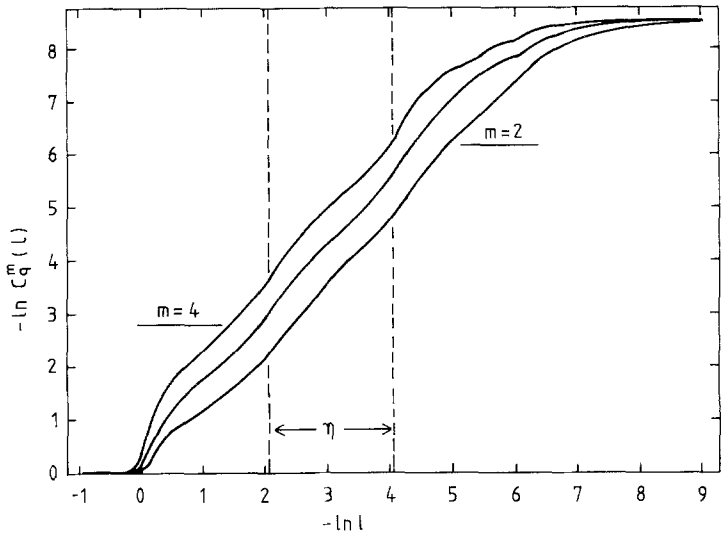


Fig. 7. Plot of $-\ln[C_q^m(l)]$ versus $-\ln l$ for $q=0$ for the embedding dimension $m=2, 3, 4$ and for the filter parameter $\eta=2$. The period of the oscillations is indicated by the two dashed lines.

If one uses for the attractor the idealization presented in Fig. 4, then $n(l)$ should be the steplike function

$$n(l)=\left[\frac{\ln(1/l)}{\eta}\right] \tag{4.11}$$

where $[x]$ is the Gauss bracket, giving the integer nearest to $x$. The steplike function $n(l)$ takes into account the fact that the number of squares $N(l)$ [Eq. (4.3)] needed to cover this idealized attractor will hardly change if $l$ is varied between $\varepsilon^n$ and $\varepsilon^{n+1}$. Inserting (4.11) in (4.3) then yields for Eq. (4.9)

$$D_0(l)=1+\frac{\ln 2}{\ln(1/l)}\left[\frac{\ln(1/l)}{\eta}\right] \tag{4.12}$$

If the function $D_0(l)$ is plotted versus $\ln l$, points of discontinuity arise due to the Gauss bracket. The distance between two neighboring points of discontinuity is $\eta$. Since the correlation function $C_0^m(l)$ preserves the topological properties of the attractor, the discontinuous points in $D_0(l)$ correspond to pieces with greater slope in $C_0^m(l)$. The periodic structure in $C_0^m(l)$ is smeared out, because the distance between neighboring lines of the

$n$th-order attractor are not exactly proportional to $\varepsilon^n$, but vary, which can be seen, for example, in Fig. 7. The amplitude of the oscillations becomes smaller for decreasing values of $\eta$.

## 5. CALCULATION OF THE GENERALIZED DIMENSION $D_q$

The generalized dimension $D_q$ is defined as[1]

$$D_q = \frac{1}{q-1} \lim_{l \to 0} \frac{\ln(\sum_{i,j} (p_{i,j}(l))^q)}{\ln l} \tag{5.1}$$

where $p_{i,j}(l)$ denotes the probability that the trajectory intersects the small square

$$S_{i,j} = [x_i - \tfrac{1}{2}l, x_i + \tfrac{1}{2}l] \times [z_j - \tfrac{1}{2}l, z_j + \tfrac{1}{2}l]$$

We take the $x_i$ and $z_j$ to be equally distributed with distance $l$. The generalized dimension of the logistic map [Eq. (2.1)] is known to be[1]

$$\bar{D}_q = \begin{cases} 1 & \text{for } q \leqslant 2 \\ \dfrac{q}{2(q-1)} & \text{otherwise} \end{cases} \tag{5.2}$$

The probability $p_{i,j}(l)$ is approximated by

$$p_{i,j}(l) \simeq \rho(x_i, z_j) l^2 \tag{5.3}$$

Using the $n(l)$th-order invariant density, this yields the following form:

$$p_{i,j}(l) \simeq 2^{-n(l)} \bar{\rho}(x_i) \sum_{m=1}^{2^{n(l)}} \delta_{v_m^{(n)}(x_i), z_j} l^2 \tag{5.4}$$

where

$$\delta_{v_m^{(n)}(x_i), z_j} = \begin{cases} 1/l & \text{if } v_m^{(n)}(x) = z \quad \text{for a point } (x, z) \in S_{i,j} \\ 0 & \text{otherwise} \end{cases} \tag{5.5}$$

The explicit form of the functions $v_m^{(n)}(x)$ is given in Eq. (2.8). The sum in Eq. (5.1) then reads

$$\sum_{i,j} (p_{i,j}(l))^q = \sum_{i,j} \left\{ 2^{-n(l)} \bar{\rho}(x_i) \sum_{m=1}^{2^{n(l)}} \delta_{v_m^{(n)}(x_i), z_j} l^2 \right\}^q \tag{5.6}$$

As long as the attractor is self-similar, the $\delta$-functions

$$\delta_{v_{m_1}^{(n)}(x_i),\, z_j} \quad \text{and} \quad \delta_{v_{m_2}^{(n)}(x_i),\, z_j}, \quad m_1 \neq m_2$$

give contributions from different squares $S_{i,j}$ only. Therefore the $j$ summation yields

$$\sum_{i,j} (p_{i,j}(l))^q = \sum_i 2^{n(l)} (2^{-n(l)} \bar{\rho}(x_i) l)^q \tag{5.7}$$

Inserting this into Eq. (5.1) gives

$$D_q = \frac{1}{q-1} \lim_{l \to 0} \frac{\ln(\sum_i (\bar{\rho}(x_i) l)^q) + (1-q) n(l) \ln 2}{\ln l}$$

$$= \bar{D}_q + \frac{\ln 2}{\eta} \tag{5.8}$$

Therefore the $q$ dependence is not affected by the filter. Formula (5.8) is valid if $\eta$ is greater than the Liapunov exponent ln 2.

In Fig. 8 the dimension $D_q$ is depicted versus $q$. The straight lines are derived from Eq. (5.8) and the points are calculated by the correlation function numerically.[4] Line 2 corresponds to $\eta \to \infty$ ($\varepsilon = 0$) and line 1 to $\eta = 1$ ($\varepsilon \simeq 0.37$).

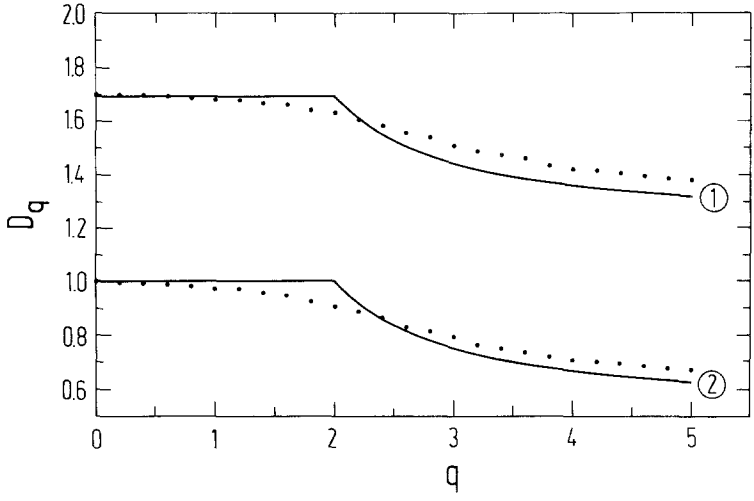


Fig. 8. Plot of $D_q$ versus $q$. The straight lines are the theoretical curves and the points are calculated by the correlation method.[4] Curve 1 is calculated for $\eta = 1$ and curve 2 for $\eta \to \infty$.

## 6. GENERALIZATION FOR AN ARBITRARY ONE-DIMENSIONAL MAP

Let $h$ be an arbitrary one-dimensional map, for which the iteration $x_{i+1} = h(x_i)$ gives a chaotic time series. We consider the system

$$\begin{pmatrix} x_{i+1} \\ z_{i+1} \end{pmatrix} = \mathbf{G}_h((x_i, z_i)) = \begin{pmatrix} h(x_i) \\ \varepsilon z_i + h(x_i) \end{pmatrix} \tag{6.1}$$

The invariant density is derived in the same way as in Section 2. Let the solutions of the equation $h(x') = x$ be given by

$$h(g_{h,j}(x)) = x, \qquad j = 1, \ldots, m \tag{6.2}$$

where $g_{h,j}$ is one of the $m$ different branches of the inverse of the function $h$. The index $h$ is added to distinguish the functions from those of Section 2. By the Frobenius–Perron equation one obtains the equation

$$\rho(x, z) = \sum_{j=1}^{m} \frac{\chi_j(x)}{\varepsilon |h'(g_{h,j}(x))|} \rho\left(g_{h,j}(x), \frac{z - x}{\varepsilon}\right) \tag{6.3}$$

where $\chi_j$ is the characteristic function, which is 1 if $g_{h,j}(x)$ is real and 0 otherwise. Let $\bar{\rho}_h(x)$ be the one-dimensional invariant density of the equation $x_{i+1} = h(x_i)$. For $\varepsilon = 0$ one obtains as a solution

$$\rho^{(0)}(x, z) = \bar{\rho}_h(x)\, \delta(z - x) \tag{6.4}$$

Using the same procedure as in Section 2, one gets the representation

$$\rho^{(n)}(x, z) = \sum_{j_1, j_2, \ldots, j_n = 1}^{m} \theta_{j_1, j_2, \ldots, j_n}(x) \times \delta\left(z - x - \sum_{i=1}^{n} \varepsilon^i g_{h,j_i}(g_{h,j_{i-1}}(\ldots(g_{h,j_1}(x))\ldots))\right) \tag{6.5}$$

The functions $\theta_{j_1, j_2, \ldots, j_n}(x)$ are derived by doing the iterations which give $\rho^{(n)}$. Since we are interested in the topological structure of the attractor only, their values for given argument $x$ are not important. The zeros of the arguments of the $\delta$-functions give the attractor of $n$th order. If $\varepsilon$ is small, the $n$th-order attractor converges to a self-similar structure for $n \to \infty$. The zeroth-order attractor is given by the line(s) $\gamma_h^{(0)} = \{(x, z) \mid z = x,\ \bar{\rho}_h(x) \neq 0\}$ and the $n$th-order attractor is given by the curve(s) $\gamma_h^{(n)} = \{\mathbf{G}_h^n((x, z)) \mid (x, z) \in \gamma_h^{(0)}\}$. If $\gamma_h^{(0)}$ consists of $k$ disconnected lines, $\gamma_h^{(n)}$ consists of $k$ disconnected curves, each arranged in a self-similar pattern in the $z$–$x$ plane for small $\varepsilon$.

Provided $k$ is finite, the following considerations will hold. From the representation of the invariant density, we know that the attractor is self-similar; therefore, we can use the same procedure as above to calculate the Hausdorff dimension. If squares of length $l$ are taken to cover the $n(l)$th-order attractor, where $n(l)$ is determined from Eq. (4.2), they will cover the attractor of the system (6.1), too. The number of squares needed to cover the $n(l)$th-order attractor is proportional the total length of the curve $\gamma_h^{(n)}$, which can be estimated by linearization of Eq. (6.1). Consider the vector

$$\begin{pmatrix} \Delta x_0 \\ \Delta z_0 \end{pmatrix} = \frac{\Delta l}{\sqrt{2}} \begin{pmatrix} 1 \\ 1 \end{pmatrix} \tag{6.6}$$

tangent to the curve $\gamma_h^{(0)}$ at the point $(x_0, z_0)$ and whose length $\Delta l$ is infinitesimally small. The map $\mathbf{G}_h^n$ maps the point $(x_0, z_0)$ into the point $(x_n, z_n) = \mathbf{G}_h^n(x_0, z_0)$ and the tangent map of $\mathbf{G}_h^n$ maps $(\Delta x_0, \Delta z_0)$ into

$$\begin{pmatrix} \Delta x_0^{(n)} \\ \Delta z_0^{(n)} \end{pmatrix} = \hat{A}_{n-1} \cdots \hat{A}_1 \hat{A}_0 \begin{pmatrix} \Delta x_0 \\ \Delta z_0 \end{pmatrix} = \begin{pmatrix} a_n & 0 \\ b_n & c_n \end{pmatrix} \begin{pmatrix} \Delta x_0 \\ \Delta z_0 \end{pmatrix} \tag{6.7}$$

where the tangent map $\hat{A}$ is given by the matrix

$$\hat{A}_j = \begin{pmatrix} \partial h(x_j)/\partial x_j & 0 \\ \partial h(x_j)/\partial x_j & \varepsilon \end{pmatrix} \tag{6.8}$$

The matrix product in Eq. (6.7) is

$$\hat{A}_{n-1} \cdots \hat{A}_1 \hat{A}_0 = \begin{pmatrix} \Delta h^n(x_0) & 0 \\ \Delta h^n(x_0) + \varepsilon\, \Delta h^{n-1}(x_0) + \cdots + \varepsilon^{n-1}\, \Delta h^0(x_0) & \varepsilon^n \end{pmatrix} \tag{6.9}$$

with

$$\Delta h^j(x_0) = \frac{\partial h(x_j)}{\partial x_j} \frac{\partial h(x_{j-1})}{\partial x_{j-1}} \cdots \frac{\partial h(x_0)}{\partial x_0} \tag{6.10}$$

from which the length $\Delta l^{(n)}$ of the iterated vector $(\Delta x_0^{(n)}, \Delta z_0^{(n)})$ can be calculated. Using the definition for the positive Liapunov exponent $\lambda_h$ of the map $h$, which states that

$$\lim_{j \to \infty} \frac{1}{j} \ln(|\Delta h^j(x_0)|) = \lambda_h \tag{6.11}$$

this length can be estimated to be

$$\Delta l^{(n)} = \{(a_n\, \Delta x_0)^2 + [(b_n + c_n)\, \Delta z_0]^2\}^{1/2} \sim \Delta l\, e^{n\lambda_h}[1 + o(\varepsilon)] \qquad \text{if} \quad n \geqslant p \tag{6.12}$$

$p$ is chosen such that it fulfills the condition

$$|\Delta h^j(x_0)| \simeq e^{j\lambda_h} \qquad \text{for all} \quad j \geqslant p \tag{6.13}$$

Since $\Delta l^{(n)}$ is nearly independent of $x_0$ for $n > p$, the length of the curve $\gamma_h^{(n)}$ is given by $\Delta l^{(n)}/\Delta l$ times the length of $\gamma_h^{(0)}$. The number $N(l)$ of squares with sides of length $l$ needed to cover the $n$th-order attractor is thus estimated to be

$$N^{>}(l) \sim \frac{1}{l} \frac{\Delta l^{(n(l))}}{\Delta l} \sim \frac{e^{n(l)\lambda_h}}{l} \tag{6.14}$$

This yields the upper bound for the Hausdorff dimension

$$D_0 \leqslant 1 + \frac{\lambda_h}{\max(\eta, \lambda_h)} \tag{6.15}$$

## 7. CONCLUSIONS

We have demonstrated for the specific example of the logistic map how a filter induces self-similarity, which is responsible for the increase of the Hausdorff dimension. The procedure could be extended to arbitrary one-dimensional maps. For the system consisting of the logistic map and the filter the generalized dimension also could be calculated.

## NOTE ADDED IN PROOF

The suggestions made in Sections 9.1 and 9.2 for reaching larger Reynolds coefficients have been recently tested, using a new implementation of the code on a Connection Machine, and we briefly report on the results. So far we have made use only of the 24-bit model FCHC-6.

The first method, thickening the lattice in the fourth dimension, unfortunately does not produce the desired result. Components of the viscosity tensor which involve the fourth dimension do indeed decrease when the thickness increases. However, the components of physical interest are those which do *not* involve the fourth dimension, and these components are found to increase with the thickness. The variations are small in any case, of the order of a few percent only.

The second method, approaching a Boltzmann situation by randomly exchanging bits between parallel replicas of the FCHC lattice, was tested using from 2 to 512 replicas. The viscosity decreases and is indeed found to tend to the Boltzmann value when the number of replicas increases. This method therefore offers a hope of ultimately reaching zero viscosity.

However, the observed convergence is rather slow. This might be due to the fact that, for reasons of computational efficiency, bit shuffling was not so far fully random.

## ACKNOWLEDGMENTS

We are grateful to K. Pawelzik, M. Heise, and A. Ritter for illuminating discussions and helpful comments on the manuscript. This work has been supported by the Deutscher Akademischer Austauschdienst and by the Deutsche Forschungsgemeinschaft through the Sonderforschungsbereich 185 Frankfurt/Darmstadt.

## REFERENCES

1. H. G. Schuster, *Deterministic Chaos*, 2nd ed. (Physik Verlag, Weinheim, 1988).
2. R. Badii and A. Politi, in *Dimensions and Entropies in Chaotic Systems*, G. Mayer-Kress, ed., (Springer-Verlag, Berlin, 1986).
3. R. Badii, G. Broggi, B. Derighetti, M. Ravani, S. Ciliberto, A. Politi, and M. A. Robio, *Phys. Rev. Lett.* **60**:979 (1988).
4. K. Pawelzik and H. G. Schuster, *Phys. Rev.* **35A** (1987).
5. J. L. Kaplan and J. A. Yorke, in *Functional Differential Equations and Approximation of Fixed Points*, H.-O. Peitgen and H.-O. Walther, eds. (Springer, Berlin, 1979), p. 204.
6. P. Frederickson, J. C. Kaplan, E. D. Yorke, and J. A. Yorke, *J. Diff. Eq.* **49**:185 (1983).